

Occurrence of Defects in Laser Beam Welded Al-Cu-Li Sheets with T-Joint Configuration

André Luiz de Carvalho Higashi¹, Milton Sérgio Fernandes de Lima^{1,2*}

¹Instituto Tecnológico de Aeronáutica – São José dos Campos/SP – Brazil

²Instituto de Estudos Avançados – São José dos Campos/SP – Brazil

Abstract: *In the aerospace industry, laser beam welding has been considered as one of the most promising routes among the new manufacturing processes. Substitution of riveting by laser beam welding of aircraft structures has contributed to weight and cost savings. Concurrently, new aluminum alloys have been developed with the addition of lithium with better mechanical properties and lower density. The Al-3.5%Cu-1.1%Li alloy (AA2198) is one of these new generation alloys. However, laser beam welding of Al-alloys expectations might be greatly reduced by the occurrence of two main defects: porosity and hot cracking. Porosity is mainly caused by the entrapment of lithium gases, followed by rapid solidification. On the other hand, hot cracking happens due to the conjunction of tensile stresses, which are transmitted to the mushy zone by the coherent solid underneath, and to an insufficient liquid feeding to compensate for the volumetric changes. This work intended to contribute towards the knowledge of AA2198 welding metallurgy, utilizing a 2-kW-ytterbium-doped fiber laser. The T-joint configuration welds were performed autogenously or with the addition of an AA4047 filler ribbon. All the weld beads presented high porosity level, but with a decreasing tendency when welding from both sides. The use of the filler material could solve hot cracking problem. The best results are observed using two runs (both sides) with filler and a speed of 2 m/min and power of 1,200 W. The T-pull tensile strength obtained under these conditions was 178 MPa, which is below the tensile strength of the unwelded AA2198 sheet but higher than the AA6013 welded in similar conditions.*

Keywords: *Laser, Laser beam welding, Aluminum alloys, Aerospace.*

INTRODUCTION

In the aerospace industry, the two routes of manufacturing technologies for structures have been constantly improved. One of them is the employment of polymer matrix composite materials in aircraft structures, which has been growing over the years (Mangalgiri, 1999). The other one is the use of conventional metallic materials with enhanced mechanical and physical properties (King *et al.*, 2009). This later could be considered as a safer route due to the very large experience of metallic alloys engineering use.

The rising competition between composites and metals took the aluminum alloys producers to develop, jointly with aircraft manufacturers, lighter alloys, with high mechanical strength and high damage tolerance. The aluminum-copper-lithium alloy AA2198 is an example of these new generation

alloys. Typically, the AA2198 alloy composition is 3.2% Cu and 1.0% Li, falling in the Al solid solution above 500 °C. Aging at lower temperatures promotes the formation of intermetallics responsible by strengthening effect (Bordesoules, 2007).

In addition to these new alloys, materials-joint techniques have been improved aiming at the reduction of weight, costs, and lead-time. Although the riveting process is highly automated, which is largely used by aircraft manufacturers, this process reached its development potential limit, and no significant advances in productivity nor in weight reduction can be expected. Thus, many joint techniques that could promote significant changes to the production process were considered, focusing on the specific needs of the aerospace industry, adding low weight and mechanical properties suitable with structural demands during aircraft lifetime operation. Among the available welding processes, friction stir welding (FSW) and laser beam welding (LBW) have presented advances over the past years, becoming attractive for the aerospace industry worldwide.

Received: 11/07/12 Accepted: 04/09/12

*author for correspondence: msflima@yahoo.com.br

Trevo Coronel Aviador José Alberto Albano do Amarante, 1 – Putim
CEP 12.228-001 São José dos Campos/SP – Brazil

LBW already found its place in industrial production, with a market in full expansion. Initially, the automotive industry developed LBW processes for sheets of different thicknesses prior to forming, which are called tailored-blanks welding, and then body-in-white laser welding. The portfolio of available flat and shaped products includes aluminum and magnesium alloys, presenting productivity and welding quality gains (Pallett and Lark, 2001).

Afterwards, the aerospace structure manufacturers began to substitute some riveted panels by laser-welded ones. The utilization of laser as a welding process allows not only weight reductions, but also the development of optimized panels, decreasing the manufacturing lead-time. If compared to the typical riveting speeds (200 to 400 mm/min), the laser welding clearly shows itself more productive, reaching speeds exceeding 6 m/min. Even with more rigorous inspections and process control, it is still profitable. Furthermore, the structure become less susceptible to corrosion, since holes in the skin are avoided and gaps in butt joints are eliminated (Rötzer, 2007).

In spite of these advantages, LBW like other fusion methods is subject to common metallurgical problems, such as hot cracking and porosities. The control of welding defects is of utmost importance to control the mechanical properties under the extreme conditions aerospace materials are subjected to. Two of the major problems in fusion welding of aluminum alloys are related to porosity and hot cracks. These problems will be further analyzed.

Porosities are intrinsically related to the weld, occurring due to a large number of factors: alloy composition, surface contaminants, improper gas shielding, keyhole collapse, and hydrogen release. In case of alloys with highly volatile elements, such as Li in the present case, boiling could also happen. Pores in Al-Li welds beads had been previously reported (ASM, 1993) as a result of hydrogen contamination leading to interdendritic microporosity.

Hot cracking, also known as solidification cracking, is one of the major defects that can occur during solidification of metallic alloys. This is the result of inadequate melt feeding initiating micropores and severe deformation leading to the opening and propagation of such defects. This type of imperfection appears at the end of the solidification when the solid fraction is high (Piwonka and Flemmings, 1966). A large solidification interval leads to a high under pressure at the dendrite roots increasing the tendency to hot cracking.

The cracking susceptibility coefficient proposed by Clyne and Davies (1981) is formulated as the ratio between the vulnerable time period (t_v), and the time available for stress-

relief process (t_R), i.e. the time spent in the interdendritic feeding stage defined as the interval between 40 and 90% solid fraction. Equation 1 presents the hot cracking susceptibility (HCS) followed by Clyne and Davies (1981).

$$HCS = \frac{t_v}{t_R} = \frac{t_{99} - t_{90}}{t_{90} - t_{40}} \quad (1)$$

Since the solid fraction is a function of temperature and alloy composition, the modification of the liquid composition is a suitable way to decrease the vulnerable time. This is usually accomplished when an eutectic forming compound is added to the weld. For example, it is well known that silicon reduces t_v in aluminum alloys because the solidification interval is reduced and the fraction of the eutectic phase is increased.

Drezet *et al.* (2008) also proposed that hot cracking could be diminished when two laser sources are used together. The main effect of these heat sources is to create a fine equiaxed region at the middle of the weld bead, so the liquid permeability increases and the thermal gradient decreases. It has been proved that a process using two laser sources improves the high temperature toughness of the AA6013 aluminum joints (Lima *et al.*, 2001).

The use of two laser sources could be unpractical in some weld geometries, but using two weld runs could reduce the thermal gradient. In the case of T-joint configuration, typical of an aircraft panel, two runs could be envisaged: one at the joint between skin and stringer and another in the opposite face. For this, two challenges must be attained: the laser beam must be very accurately positioned at the interface between the pieces and at a correct angle, and the filler material must be inserted in some way it is not obstructing the beam. Therefore, the first challenge is going to be accomplished by the high quality fiber laser beam. The second one could be overcome by using a filler ribbon instead of a filler wire and by inserting this ribbon directly at the joint intersection.

This work intended at contributing to the study of weldability of the AA2198 alloy using a fiber laser. The experimental results of the weldability are missing in the literature and the use of a new laser source, fiber laser, could produce a new insight on the matter. The weld geometry is similar to that of a stringer-skin T-joint both autogenous and filled with an Al-Si alloy ribbon.

MATERIALS AND METHODS

A 1.6 mm thick aluminum alloy AA2198-T851 sheet was utilized in this work. Its composition is shown in Table 1. The sheet was cut in coupons with 30 x 100 mm dimensions. For

Table 1. AA2198 alloy composition in weight percent (Al as the balance).

Element	Cu	Mg	Li	Ag	Zr	Mn	Si	Zi	Ti	Fe	Other
% wt.	3.50	0.80	1.10	0.50	0.18	0.50	0.08	0.35	0.10	0.10	0.15

Table 2. AA4047 alloy composition in weight percent.

Element	Al	Cu	Mg	Mn	Si	Fe
% wt.	87.83	0.0015	0.001	0.01	11.89	0.252

welds performed with filler, the aluminum alloy AA4047 was utilized and its composition is shown in Table 2. Wires of 1.0 mm in diameter were cold rolled to ribbons of 1.6 mm of width and 0.2 mm thickness. The ribbons were placed between the sheets and firmly attached using a bench vise in a T-joint configuration as depicted in Fig. 1. Based on previous studies, the angle between the laser beam and the skin surface was fixed at 16°.

A 2-kW-continuous wave fiber laser produced by IPG Co. (USA) was used. The laser radiation is generated in a 50 mm diameter fiber doped with ytterbium. The doped fiber is connected to a process fiber with 100 mm diameter, which is then connected to an Optoskand processing head. The focal length was 157 mm with a minimum spot diameter at the focus of 100 mm.

Pure helium gas at 30 l/min flow rate was used to protect the surface against oxidation. The protection gas was delivered through a rounded copper tube of 2 mm internal diameter directly over the irradiated area (Fig. 1). A computer numerical control (CNC) table carries out the sample movement. Right before welding, the sample surface was grounded with a

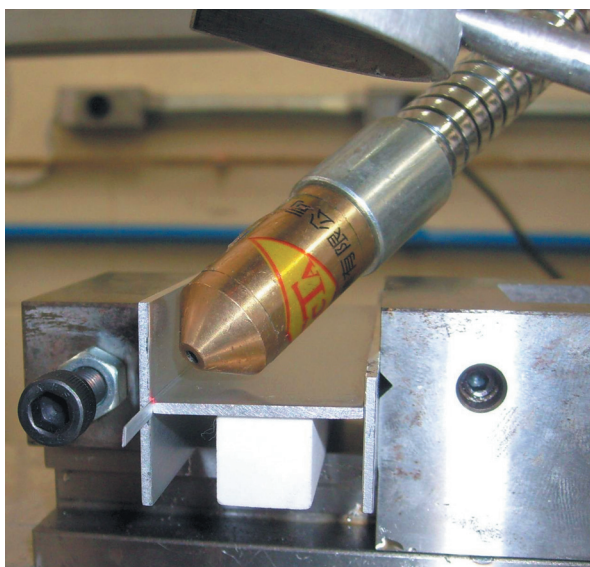


Figure 1. Experimental setup showing aluminum parts fixed at the bench. The white block is an alumina calibrated support, and the rounded nozzle is responsible for gas shielding.

SiC 600 paper to remove oxidation and then washed with distilled water and ethanol.

Microstructural analyses were carried out using optical microscopy (OM) and scanning electron microscopy (SEM). The OM is a reflected light Reichert Polyvar 2 (Germany) equipped with acquisition system and image processing software. The SEM is a Zeiss Model LEO 435 Vpi (Germany).

The equipment for mechanical tests was an MTS 810 tensile machine (USA) having a loading cell with 250 kN capacity. The mechanical testing was carried out in T-pull mode, as described in Fig. 2. The load is realized by pulling the stringer at constant speed of 1.0 mm/min. The sample dimensions for T-pull testing were: 3(W)x3(H)x2(L) cm.

In order to understand the thermal and mechanical behaviors during welding, a finite element analysis was performed using the ESI-Group Sysweld® software (France). As the physical properties of AlCuLi alloy are missing in the literature, the simulation had been performed using the constants of an AlSiMg alloy class AA6061. One and two-sided welding conditions were simulated in autogenous condition. In order to reproduce experimental conditions, the simulated sheets were rigidly attached to the borders, and the time between the start of each weld, for the two sides welds, was ten seconds. The mechanical formalism is based on Von Mises strain and stresses (Wikipedia, 2012).

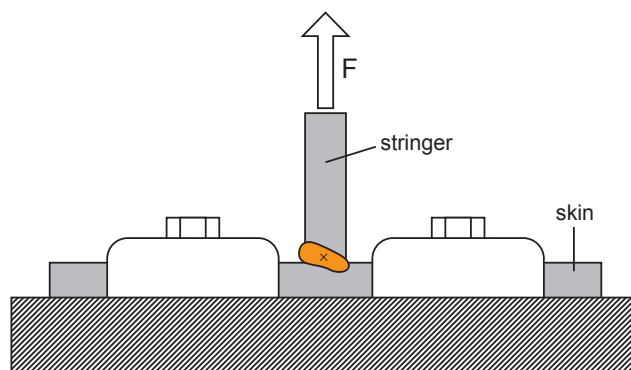


Figure 2. T-pull mechanical testing schematics. The skin part of the joint is attached to a table with two screws-fixed clips. The force (F) is applied parallel to the stringer direction.

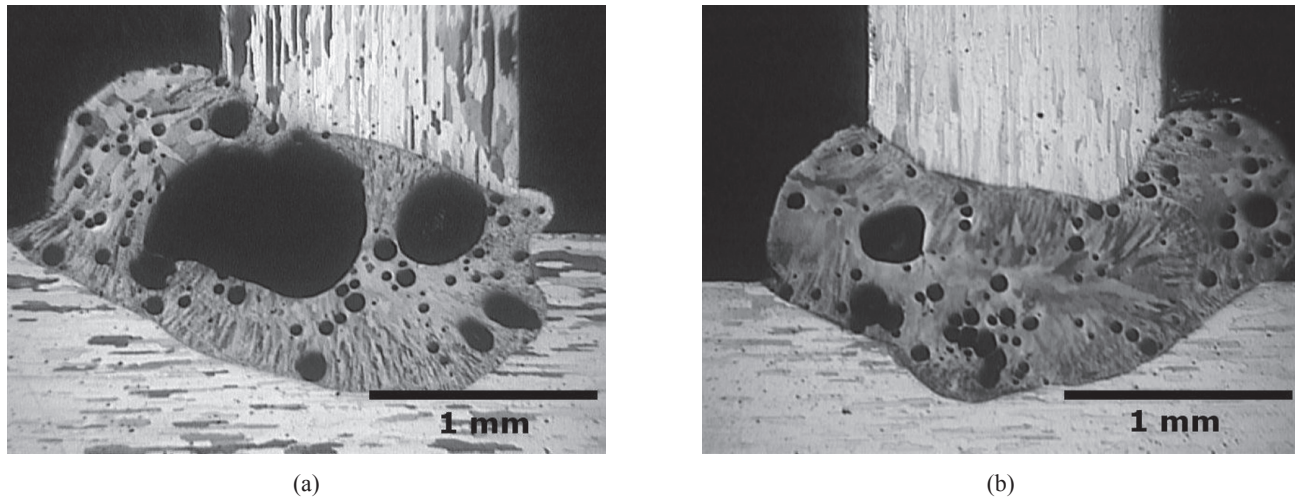


Figure 3. Optical micrographic images of the weld seams. (a): one side beam, condition: one run – 1,400 W/3 m/min. (b): two runs – 1,200 W/4 m/min.

After a number of free trials, some experimental conditions have been retained for a detailed study. Table 3 presents the experimental conditions for the welds, where the run could be one or two depending if one or both sides were exposed to the beam. The heat input is the ratio of power per speed for each run.

RESULTS AND DISCUSSION

In the present work, the parameters affecting the heat input provided by the laser, speed (v) and power (P) were studied. In general, the combination of P and v of the welds generated weld beads of reasonably similar dimensions. For the T-joint configuration, the laser beam came from one (Fig. 3a) or two sides (Fig. 3b), however the welded zones were always asymmetric. All samples presented epitaxial growth of grains from the base/molten metal interface towards the bead top. The slower solidification next to

the base material promoted the coarser dendrite formation with columnar structure. Near the bead top, where cooling rate was higher, the grains had not preferential orientation providing equiaxial growth of finer dendrites.

As can be seen in Fig. 3, a great quantity of pores is presented in all weld beads. Some of them presented large toes (Figs. 3a and 3b), which can be explained by the large number of pores within them. Microporosity as much as macro-porosity were present in the welded zone, indicating one or more mechanisms of pore formation. Pores are verified all along the extension of the welds, however the volume fraction of pores does not have statistical meaning because of large variations in their density from one cross-section to the other.

These pores are mainly linked to the lithium degassing during melting and are frequently associated with poor weldability of Al-Li alloys. The welds with both side seams, as presented in Fig. 3b, showed smaller pores, indicating that the Li vapor had more time to leave the molten pool. Other possible sources of porosity to be considered are surface and gas contaminants. The current careful control of surface finishing decreases the possibility of surface contaminant, thus having a minor role in the porosity. Additionally, other types of aluminum alloys had been welded in the same experimental conditions (Siqueira *et al.*, 2012), including use of the bench vise and the gas nozzle as presented in Fig. 1. Usually, these welds present only few small pores. Therefore, it is much likely that pores are due to Li degassing and, to an unknown extent, to hydrogen nucleation (ASM, 1993).

Figure 4 presents a closer look of a separate pore cross-section using secondary scanning electron microscopy. It

Table 3. Process parameters.

Power (W)	Speed (m/min.)	Heat input (J/mm)	Condition
1,200	2	36	Autogenous/two runs
1,200	2	36	Autogenous/one run
1,200	2	36	With filler/two runs
1,200	2	36	With filler/one run
1,400	3	28	Autogenous/one run
1,400	3	28	With filler/one run
1,400	3	28	With filler/one run
1,200	4	18	With filler/two runs

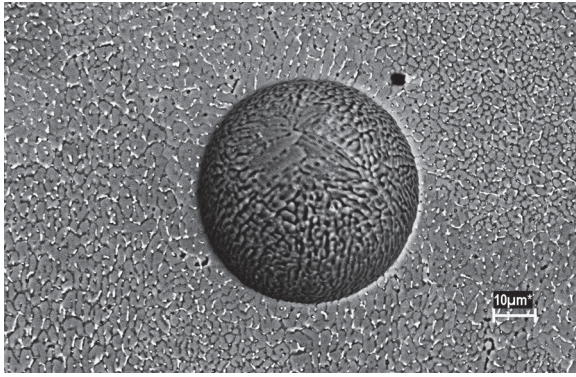


Figure 4. Pore observed at condition: with filler, 1,200 W, 2 m/min, one run.

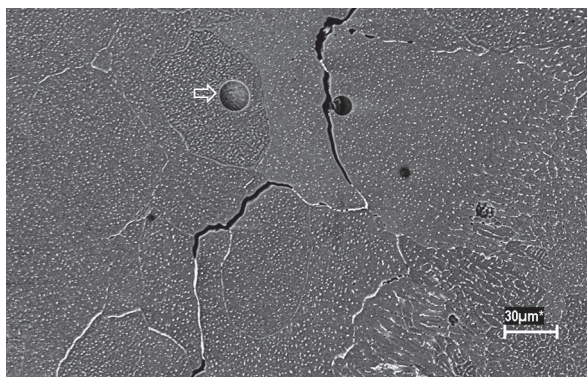
can be seen that the porosity is perfectly spherical with inner surface finely decorated with dendrite arms. The region around the observable circle presents fine equiaxed grains with epitaxial growth from the disc to the surroundings. This observation indicates that pores inoculate the liquid with low-energy nucleation sites that help fine grain growth. In Fig. 5a it could be seen a pore in the middle of an isolated grain (arrow). Page and Sear (2006) also showed that pores are preferred sites for heterogeneous nucleation of new phases. The same mechanism of metal nucleation around pores is also observed in metal foams. Duarte and Banhart (2000) verified the nucleation of alpha grains around pores in the foam-processed aluminum alloys classes AlSi7 and AA6061. As grain refiners, the small pores could increase the weld seams toughness, particularly in high temperatures in which hot cracks appears. However, the large pores observed here act as stress concentrators and probably hide the positive effects of fine pore inoculation.

The use of Al-Si filler seems to decrease the tear tendency in the fusion zone. The welds performed with laser power of

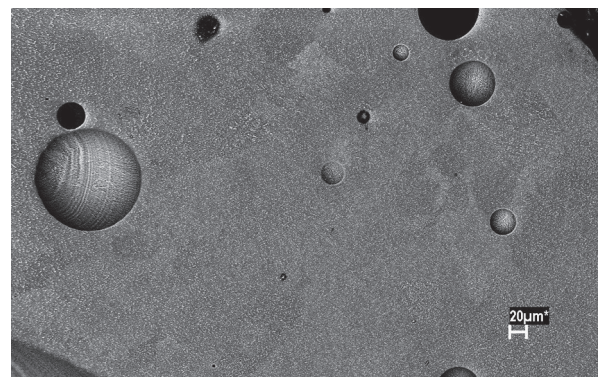
1,200 W and 2 m/min speed did not present hot cracking with filler addition, unlikely the autogenous condition. Figures 5a and 5b show the autogenous weld and weld with the filler, respectively. Thus, the HCS was reduced to this condition with the addition of the AA4047 filler ribbon. According to the current theories (Campbell, 2003), the chemical composition is changed reducing the vulnerable solidification interval. It is not possible to accurately measure the actual composition of the welded zone using the energy-dispersive X-ray spectroscopy of the scanning electron microscope (SEM-EDS), since many alloying elements were well-below 1 weight percent and the second most important alloying element (Li) was too light to be detected. Nevertheless, semiquantitative chemical analyses were performed, and are presented in Fig. 6 for two samples with Al-Si additions. It could be seen that silicon distribution is approximately homogeneous in all areas, but at the bottom region, next to the skin, called “2” in Fig. 6. The accumulation of Si in these regions could be explained due to the absence of high liquid convection fluxes in lateral regions of the weld pool.

Through SEM-EDS imaging analyses, the composition of two side-welded beads was obtained. The content of silicon of the filler wire (which composition is approximately the eutectic Al-12% Si) was diluted in the bead during welding. The molten metal convection flows permitted the solutes to dilute out over the entire bead during welding.

A possible way to study the influence of chemical composition on hot cracking is to compare the ratio of vulnerable to stress-relief times, as presented in Eq. 1. With regards to the same cooling conditions, one could compare the temperature interval, related to t_v and t_R , between an alloy composed Al-2.9%Cu-1.1%Si (Fig. 6) and another with Al-3.5%Cu. Thermocalc (1994) computations provided the results presented in Table 4, and as can be seen the HCS drops



(a)



(b)

Figure 5. Hot cracking in the welded zones. (a): autogenous weld seam, condition of 1,200 W/2 m/min. (b): weld seam with filler, free of cracking, condition of 1,200 W/2 m/min.

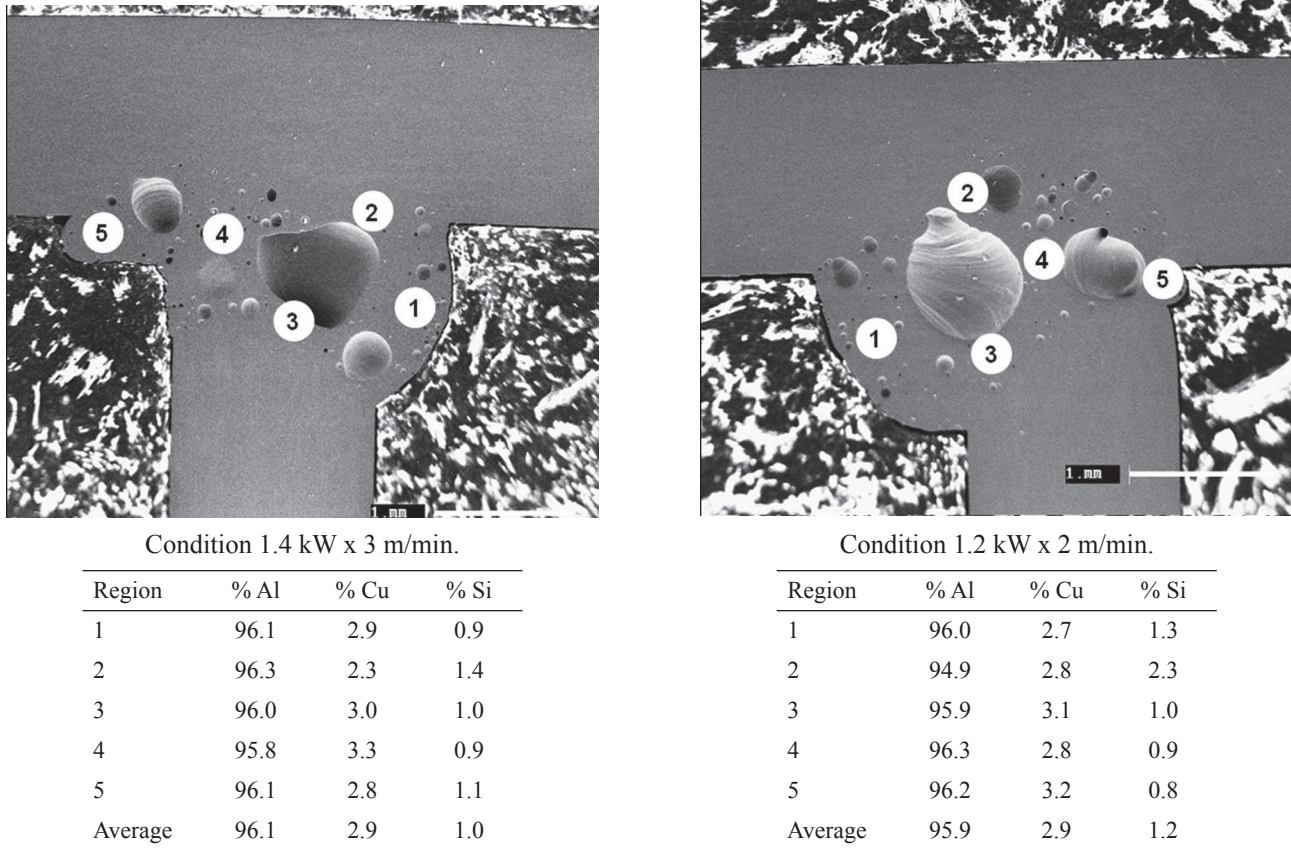


Figure 6. Energy-dispersive X-ray spectrometry chemical analyses of two weld beads, filled with the Al-Si ribbon. The tables below each picture indicate the chemical composition for each region.

from 0.92 to 0.77 when using filler material. These numbers are only indicative because the real solidification interval depends on the actual melt composition and cooling conditions.

As HCS is linked to the ratio of the solidification intervals (Table 4) and the mechanical strains during the final stages of solidification, then one needs to evaluate the thermomechanical evolution during welding by computer simulation. The finite element modeling was carried out using the Sysweld® software for the T-joint welding, in similar

Table 4. Calculation of temperature intervals in different compositions. T(fs) means temperature in Kelvin at a given solid fraction. HCS: hot cracking susceptibility.

Temperature (K)	Welding with AlSi filler Al-2.9%Cu-1.1%Si	Welding without AlSi filler Al-3.5%Cu
T (fs=99%)	837.04	857.04
T (fs=90%)	869.93	887.01
T (fs=40%)	912.57	919.51
HCS (Equation 1)	0.77	0.92

HCS: hot cracking susceptibility.

conditions to the experimental setup. One-side welding temperature and mechanical response were simulated with power of 1,400 W and a speed of 3 m/min. For the simulation of two-side weld, the chosen parameters were power of 1,200 W and speed of 4 m/min. The current thermal inputs were 28 and 18 J/mm per run (Table 3), for one and two-side welds, respectively. These simulation parameters were similar to those experimentally observed in Fig. 3. Figure 7 presents data plots as a function of processing time. For the two-side welds, the second curve begins at ten seconds because the second run started at this time.

As seen in Fig. 7a, temperature versus time profile was quite similar at the beginning of the welding process. The second run, for the two-side weld, produces a second peak, which after ten seconds attains about 580 °C, approximately the *solidus* temperatures for the Al-Cu-Li and the Al-Si fillers. Indeed, the second run promotes a melt depth up to the opposite surface as shown in Fig. 3b. Since two melting periods are expected, the liquid had additional time for Li degassing in comparison to the one side run. Therefore, less porosity was obtained with two runs.

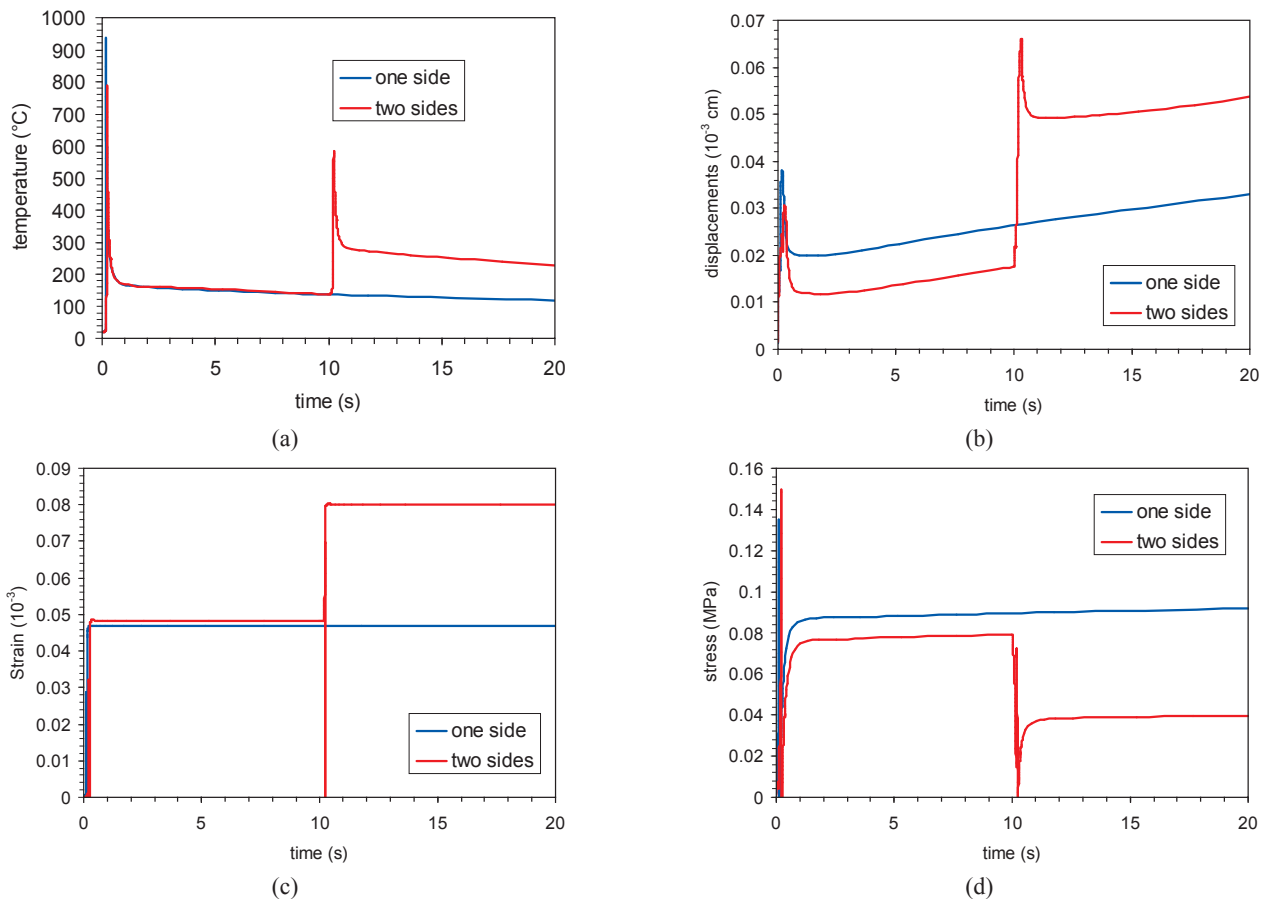


Figure 7. Simulation results. (a) temperature profile at the center of the weld, first run side. (b) displacement of a node at the middle between two sheets. (c) Von Mises strain. (d) Von Mises stresses.

The displacement (Fig. 7b) represents the shift in position during welding of a point at the centerline exactly at the interface between the sheets. The measurement position is represented by “x” in Fig. 2. As the sheets were firmly attached to the bench (Fig. 1), these movements were highly constrained leading to residual stresses. The rigid clamping had therefore influences on the strains and stresses, as shown in Figs. 7c and 7d. The calculated strain during welding attained 5×10^{-5} for the first run and about 8×10^{-5} for the second. The most important feature for cracking is the strain rate. A very high strain rate creates porosities at the root of dendrites, thus developing hot cracking (Rappaz *et al.*, 1999). The value attained at the second run was 0.02 s^{-1} . This value is very low and considered safe, at least for the AA6061 aluminum alloy (Drezet *et al.*, 2008).

The effect of different weld procedures on the mechanical stresses is presented in Fig. 7d. The low heat input of the two-side method compared to the one-side allowed a lower level of residual stress up to ten seconds. The residual stresses at ten seconds were 0.09 and 0.07 MPa, respectively. After the second run, the difference was even larger, 0.09 and 0.04 MPa.

These stress levels are very low compared to the elastic properties of aluminum alloys and thus the distortion should be very small. Indeed, the T-sets did not show distortions after welding.

All these simulation results had been developed using an AA6061 alloy database, and the filler additions had not been considered. Therefore, the results must be considered only in a qualitative way. Notwithstanding these results, it could be estimated that the T-joint with better chances to be used in applications is that with filler and two runs. Now, one need to understand if the observed massive porosity produces an unsuitable weld from the mechanical point of view.

The mechanical characterizations of the welds were presented in Figs. 8 and 9. For clarity reasons, the stress is presented in logarithm scale. Figure 8 presents a direct strain-stress curve comparison between an autogenous and filler T-joint, when welded from one side to the other. As can be seen, the curves were very similar with a plateau up to 3.2 mm elongation corresponding to the flexion of the skin sheet at low stresses. It is easy to see in Fig. 2 that the skin sheet will bend creating a three-point load scheme at the beginning of

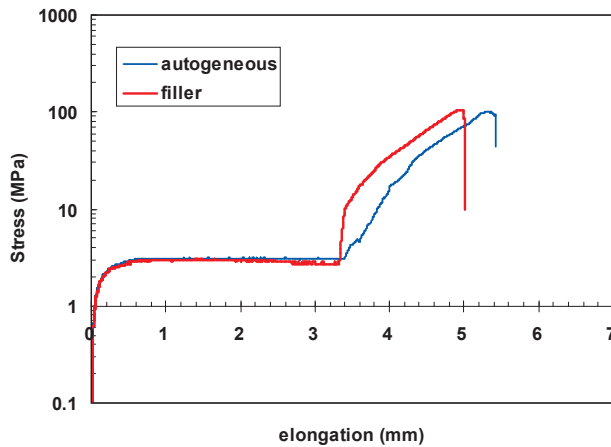


Figure 8. Comparison of the mechanical behavior between an autogeneous and filler-added welded. Conditions: one-side welded (one run), $P=1,200$ W, $v=2$ m/min.

the mechanical testing. The tensile stress and maximum elongation seems to be approximately the same, regardless the use of filler for one-run joints.

The mechanical behavior was completely different when welding from both sides (Fig. 9). Compared to the two-side autogeneous weld, the use of filler together with the double side welding increased the tensile strength from 19 to 178 MPa, and the total elongation from 4.1 to 6.3 mm. The increased toughness, more than ten times, had been linked to the chemical changing of the liquid bath, since the thermomechanical behavior (Fig. 7) was about the same.

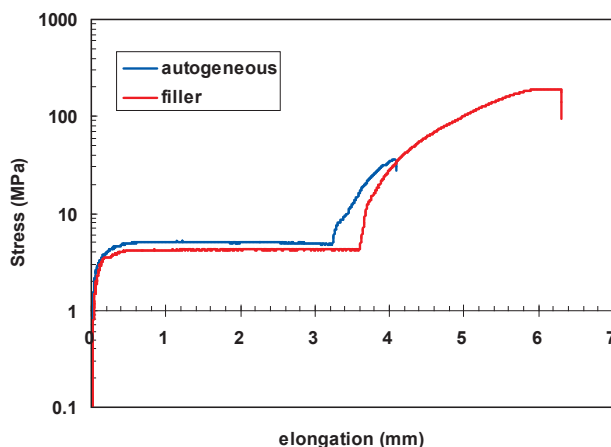


Figure 9. Comparison of the mechanical behavior between an autogeneous and filler-added welded. Conditions: both sides welded (two runs), $P=1,200$ W, $v=2$ m/min.

It is worthwhile to compare the best result obtained in the present work with the two cases. Firstly, the AA2198 sheet without welding as the maximum attainable value. Secondly,

another aerospace alloy, AA6013, welded in similar T-joint conditions, welded one-side and autogenously. These results are presented in Fig. 10.

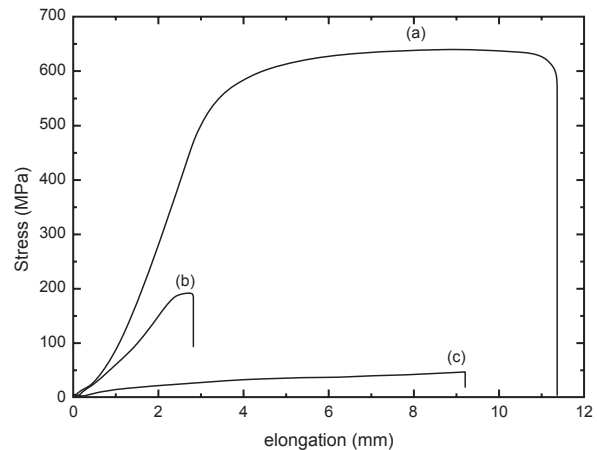


Figure 10. Comparison of the tensile mechanical behavior. Conditions: (a) unwelded AA2198 sheet (maximum attainable condition); (b) Welded on both sides (two runs), $P=1,200$ W, $v=2$ m/min; (c) AA6013 aluminum alloy autogenously welded on one side.

The AA2198 welded coupons presented lower tensile strength and total elongation in comparison to the AA2198 unwelded coupon. This is due to the stress concentrator factor caused by the weld bead.

Comparing the best results obtained in T-joint welds for AA2198 and AA6013, it could be seen that the tensile strength was much higher in the first case. The AA2198 welded coupon attained 178 MPa, compared to only 46 MPa of the AA6013 case. On the other hand, the total elongations were 9.2 from AA6013 and 2.8 mm for AA2198, indicating a hardening effect of the filler material in the present case.

CONCLUSIONS

Even with a careful control of surface preparation, all the AA2198 T-joint welds presented pores, which were linked to the degassing of Li during melting.

Adding a filler ribbon of AA4047 alloy between the parts to be joined could solve the hot cracking problem. The decrease of the vulnerable to stress relief time during solidification was pointed out as the reason, from the lower susceptibility for hot cracking.

The results from thermomechanical and chemical analyses, and tensile T-pull strength testing indicated that welded by

two runs, on both sides, and by using the filler ribbon produce tougher joints.

The welds at 2 m/min and 1,200 W under these conditions were showing most promising properties, even in comparison to T-joined autogeneous AA6013 alloy.

Because of high pore density, it is safer to consider less critical applications than the aerospace one. Depending on other results, such as fatigue behavior, the AA2198 welded parts could be used, for example, in land transportation systems.

ACKNOWLEDGMENTS

The authors thank EMBRAER for providing the aluminum sheets, *Financiadora de Fundos e Projetos* (FINEP) and *Fundação de Amparo à Pesquisa do Estado de São Paulo* (FAPESP) for partial funding.

REFERENCES

- ASM – American Society of Materials, 1993, “Metals Handbook – Volume 6: Welding, Brazing, and Soldering”, 10th ed., Metals Park (Ohio), ASM International, pp. 1392-1393.
- Bordesoules, I. *et al.*, 2007, “Trends in developments of Aluminium solutions for aerospace applications”, In: Proceedings of the European Workshop on Short Distance Welding Concepts for Airframes frames – WEL-AIR, Hamburg, 13-15 June 2007, CD-Rom.
- Campbell, J., 2003, “Castings”, 2nd ed., Oxford: Elsevier Pergamon, 332p.
- Clyne, T.W. and Davies G.J., 1975, “A Quantitative Solidification Test for Casting and An Evaluation of Cracking in Aluminium-Magnesium Alloys”, *The British Foundryman*, Vol. 68, pp. 238-254.
- Drezet, J.M. *et al.*, 2008, “Crack-free aluminium alloy welds using a twin laser process, In: 61st International Conference of the International Institute of Welding”, Graz. Safety and reliability of welded components in energy and processing industry. Graz (Austria), TU-Graz, pp. 87-94.
- Duarte, I. and Banhart, J., 2000, “A study of aluminium foam formation-kinetics and microstructure”, *Acta Materialia*, Vol. 48, pp. 2349-2362.
- King, D. *et al.*, 2009, “Advanced aerospace materials: past, present and future, Aviation and The Environment”, Vol. 3, pp. 22-27.
- Lima, M.S.F. *et al.*, 2000, “Advanced laser welding process”, European patent no. 01810986.8.
- Mangalgi, P.D., 1999, “Composite materials for aerospace applications”, *Bulletin of Materials Science*, Vol. 22, pp. 657-664.
- Page, A.J. and Sear, R.P., 2006, “Heterogeneous Nucleation in and out of Pores”, *Physical Review Letters*, Vol. 97, pp. 065701-1-065701-4.
- Pallett, R.J. and Lark, R.J., 2001, “The use of tailored blanks in the manufacture of construction components”, *Journal of Materials Processing Technology*, Vol. 117, pp. 249-254.
- Piwonka, T.S. and Flemings M.C., 1966, “Pore formation during solidification”, *Transactions of Metallurgical Society AIME*, Vol. 236, pp. 1157-1165.
- Rappaz, M. *et al.*, 1999, “A new hot tearing criterion”, *Metallurgical and Materials Transactions*, Vol. 30A, pp. 449-455.
- Rötzer I., 2005, “Laser-beam welding maker aircraft lighter”, *Fraunhofer Magazine*, Vol. 1, pp. 36-37.
- Siqueira, R.H.M. *et al.*, 2012, “Microstructural and Mechanical Characterization of Laser Welded and Heat-Treated AA6013 Aluminum Alloy”, In: Proceedings of XI Brazilian MRS Meeting, CD-Rom.
- ThermoCalc thermodynamic database, 1994, version J, Stockholm Royal Institute, Sweden.
- Wikipedia, the free encyclopedia, 2012, Von Mises yield criterion, Retrieved in June 25, 2012, from http://en.wikipedia.org/wiki/Von_Mises_yield_criterion.

